Nuclear levels in proton-unbound ^{109}I: Relative single-particle energies beyond the proton drip line

M. Petri,[1] E. S. Paul,[1] B. Cederwall,[2] I. G. Darby,[1,*] M. R. Dimmock,[1] S. Eeckhaudt,[3] E. Ganioğlu,[2] T. Grahn,[3,†] P. T. Greenlees,[3] B. Hadinia,[2] P. Jones,[3] D. T. Joss,[1] R. Julin,[3] S. Juutinen,[3] S. Ketelhut,[3] A. Khaplanov,[2] M. Leino,[3] L. Nelson,[1] M. Nyman,[3] R. D. Page,[1] P. Rahkila,[3] M. Sandzelius,[2] J. Sarén,[3] C. Scholey,[3] J. Sorri,[3] J. Uusitalo,[3] and R. Wadsworth[4]

[1]*Oliver Lodge Laboratory, University of Liverpool, Liverpool L69 7ZE, United Kingdom*
[2]*Department of Physics, Royal Institute of Technology, S-10691 Stockholm, Sweden*
[3]*Department of Physics, University of Jyväskylä, FIN-40014 Jyväskylä, Finland*
[4]*Department of Physics, University of York, Heslington, York YO10 5DD, United Kingdom*

(Received 23 April 2007; published 1 November 2007)

A level scheme has been constructed for the proton-unbound, $T_z = 3/2$ nuclide $^{109}_{53}I_{56}$ following a recoil-decay-tagging experiment using the ^{58}Ni(^{54}Fe, $p2n\gamma$) reaction at a beam energy of 195 MeV. The experiment was performed using the highly efficient JUROGAM γ-ray spectrometer in conjunction with the RITU gas-filled recoil separator and the GREAT focal-plane spectrometer. Cranking calculations are used to interpret band structures built on $\pi g_{7/2}$ and $\pi h_{11/2}$ states in a weakly deformed, triaxial nucleus.

DOI: 10.1103/PhysRevC.76.054301 PACS number(s): 27.60.+j, 21.10.Re, 23.20.Lv

I. INTRODUCTION

Heavy nuclei with exotic values of neutron-proton ratios provide a fertile testing ground for nuclear models. For example, proton-rich nuclei in the $A \sim 100$ region, close to the $N = Z = 50$ double shell closure, are of great interest, because valuable information on single-particle energies and residual interactions with respect to the doubly magic ^{100}Sn "core" can be extracted. In this regard, it is of paramount importance to follow single-particle energies systematically in nuclei ever closer to this doubly magic nucleus. Another intriguing feature of this mass region is the predicted octupole collectivity in nuclei close to $N = Z = 56$ (^{112}Ba) [1]. For this particle number, a deformed octupole shell gap occurs, and both proton and neutron orbitals that differ by $\Delta j = \Delta \ell = 3$, namely, $h_{11/2}$ and $d_{5/2}$ states, are at the nuclear Fermi surface. Such orbitals are required for enhanced octupole collectivity [2].

γ-ray transitions in the proton-unbound ^{109}I nucleus were first proposed in Ref. [3]. However, in subsequent work [4] discrepancies of the γ-ray transitions assigned to ^{109}I were found. The present data, with a significant increase in the statistics over the previous experiments, have now allowed a resolution of the conflict, and a new level scheme has been built for ^{109}I. Cranked Woods-Saxon calculations suggest a weakly deformed, triaxial shape for ^{109}I, and they are used to interpret the observed structures. In particular, the relative energies of the proton $g_{7/2}$ and $h_{11/2}$ orbitals have been established in ^{109}I, a nuclide beyond the proton drip line.

II. EXPERIMENTAL DETAILS

The present experiment was carried out at the JYFL accelerator facility at the University of Jyväskylä, Finland, using the extremely sensitive recoil-decay-tagging technique [3,5]. States in ^{109}I were populated using the ^{58}Ni(^{54}Fe, $p2n\gamma$) fusion-evaporation reaction. The $^{54}Fe^{10+}$ ions, accelerated by the JYFL K130 cyclotron to a near-barrier energy of 195 MeV, were used to bombard a target consisting of a 1 mg/cm^2 self-supporting foil of isotopically enriched (99.8%) ^{58}Ni. The irradiation time was around 5 days with an average beam intensity of 5 pnA.

Prompt γ rays emitted from the recoiling ($v = 0.036c$) residues were detected at the target position by the JUROGAM γ-ray spectrometer, which consisted of 43 Eurogam-type [6] escape-suppressed high-purity Ge detectors. The angular coverage with respect to the beam axis is from 72° to 157° in six different rings. In this configuration, the JUROGAM spectrometer has a measured photopeak efficiency of $\approx 4.1\%$ at 1.3 MeV. The fusion-evaporation residues were separated in flight from the primary beam particles by the gas-filled recoil separator RITU (Recoil Ion Transport Unit) [7,8] and implanted into the double-sided silicon strip detector (DSSD) of the GREAT (Gamma Recoil Electron Alpha Tagging) focal-plane spectrometer [9].

The signals from all the detectors were recorded using the total data readout (TDR) acquisition system [10], which has been developed for the GREAT spectrometer and comprises a triggerless system in which all channels run independently. All the signals were provided with an absolute "time stamp" from a global 100 MHz clock to an accuracy of 10 ns. Event reconstruction involves a software trigger as well as spatial and temporal correlations. For this reconstruction and consequent analysis of the data, the GRAIN package [11] was used.

The present experiment used a nearly symmetric reaction, which in the past had caused problems for beam/recoil discrimination in the RITU spectrometer. However, several improvements recently implemented in RITU, in

*Present address: Department of Physics and Astronomy, University of Tennessee, Knoxville, Tennessee 37996, USA.
†Present address: Oliver Lodge Laboratory, University of Liverpool, Liverpool L69 7ZE, United Kingdom.

 ©2007 The American Physical Society

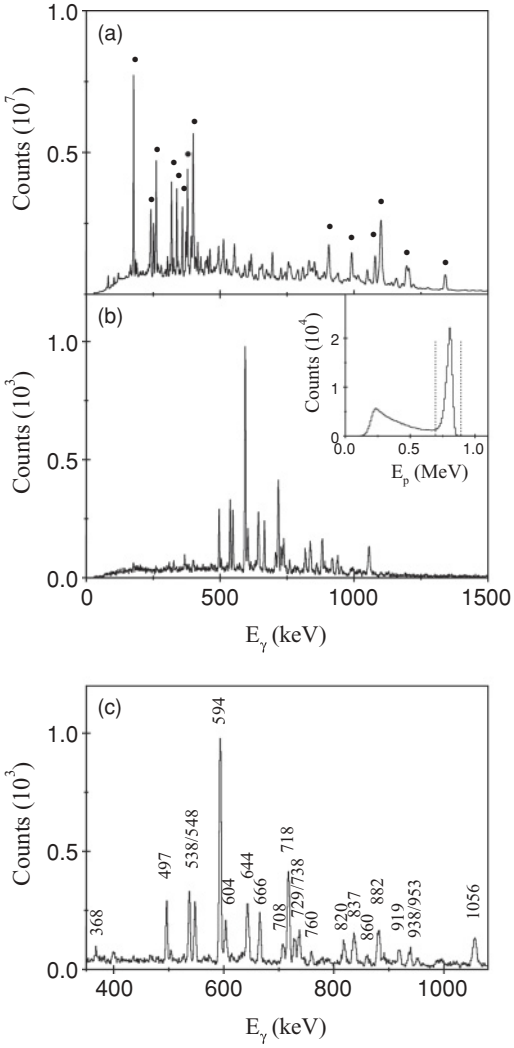

FIG. 1. (a) Prompt γ-ray spectrum (1 keV/channel) correlated with any recoil detected at the focal plane of RITU. Peaks marked with filled circles are strong transitions in the dominant exit channel, ^{109}Sb. (b) Prompt γ-ray spectrum (1 keV/channel) correlated with the ground-state proton decay of ^{109}I. The inset of (b) shows the decay-energy spectrum recorded by the DSSD for a 300 μs correlation time between a recoil implantation and its subsequent decay. The strong peak in the decay spectrum corresponds to the 813 keV ground-state proton decay of ^{109}I, while the tail on the left consists of escaped protons and β particles. The dotted lines define the energy gate in the time-correlated decay spectrum for which the prompt γ rays in JUROGAM have been assigned as transitions in ^{109}I. (c) Same as (b), but with an expanded energy axis and with the assigned ^{109}I transitions labeled by their energies.

conjunction with energy loss and time-of-flight information from the GREAT multiwire proportional counter (MWPC) and DSSD, resulted in the first observation of γ rays in ^{106,107}Te [12,13]. These nuclei were produced in the exactly symmetric ^{54}Fe+^{54}Fe and nearly symmetric ^{52}Cr+^{58}Ni reactions, respectively, with cross sections as low as 25 nb for ^{106}Te. In addition, results from the present work for ^{110}Xe have recently been documented in Ref. [14].

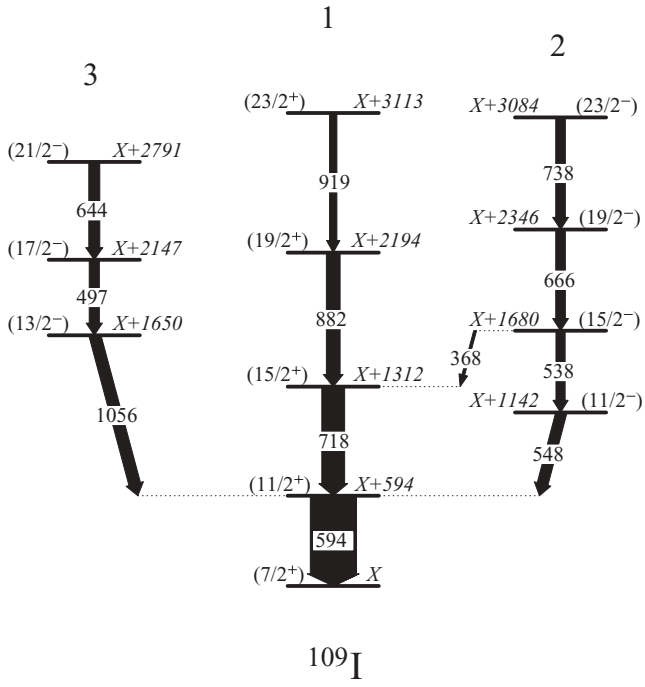

FIG. 2. Level scheme deduced for ^{109}I. Level and transition energies are labeled in keV. The widths of the arrows are proportional to the relative γ-γ coincident transition intensities, as derived from a global fit to the proton-correlated γ-γ matrix, and hence different from those given in Table I. The level energies are given relative to the lowest $(7/2^+)$ state, which is probably not the ground state. The tentative spin-parity assignments are discussed in the text.

III. RESULTS

Prompt γ rays correlated with any recoiling nucleus detected at the focal plane of RITU are shown in Fig. 1(a). The dominant exit channel in the ^{58}Ni +^{54}Fe reaction at 195 MeV involves three-proton evaporation, leading to $^{109}_{51}$Sb [15]. The ground-state proton decay of ^{109}I has previously been characterized by a decay energy of 813(4) keV, with a half-life of 100(5) μs, and a branching ratio of $\approx$ 100% [16,17]. Very recently, a weak α branch (10^{-4}) was observed for ^{109}I [18], and the proton-decay lifetime was measured as 93.5(3) μs. The present data yield a lifetime of 92(1) μs for the proton decay.

From a total of approximately 1.4×10^5 protons assigned to the ground-state decay of ^{109}I, using a search time of 300 μs, only 5×10^4 were correlated with a JUROGAM event. This however represents a tenfold increase over previous work [4]. γ rays from the present proton-correlated events are shown in Fig. 1(b). The production cross section for ^{109}I was estimated to be $\sim 10\,\mu$b. Prompt coincident γ rays correlated with the ^{109}I proton radioactivity were sorted into a symmetric γ-γ matrix in order to build a level scheme. The level scheme for ^{109}I, deduced from γ-γ coincidence relationships and γ-γ coincident intensities [19], is shown in Fig. 2, where three band structures are labeled. Properties of the γ-ray transitions assigned to ^{109}I are listed in Table I, including several which have not been placed in the level scheme of Fig. 2. Excess intensity in the singles over the γ-γ coincidences of the 538

TABLE I. Properties of γ-ray transitions assigned to ^{109}I. Not all transitions could be placed in the level scheme of Fig. 2. The relative intensities and angular-intensity ratio R were extracted from proton-correlated singles spectra.

E_γ (keV)	I_γ (%)	R	Multipolarity	Assignment	Band
368.1(3)	<5			$(15/2^- \rightarrow 15/2^+)$	$2 \rightarrow 1$
496.6(2)	20(1)	1.2(2)	$E2$	$(17/2^- \rightarrow 13/2^-)$	3
537.8(2)[a]	27(1)[a]	1.0(1)	$E2$	$(15/2^- \rightarrow 11/2^-)$	2
548.2(2)	23(1)	1.0(1)	$E1, \Delta I = 0$	$(11/2^- \rightarrow 11/2^+)$	$2 \rightarrow 1$
593.9(2)	$\equiv$ 100(3)	$\equiv$ 1.0(1)	$E2$	$(11/2^+ \rightarrow 7/2^+)$	1
603.8(2)	17(1)				
643.7(2)[a]	33(2)[a]	1.2(2)	$E2$	$(21/2^- \rightarrow 17/2^-)$	3
666.1(2)	23(1)	1.1(1)	$E2$	$(19/2^- \rightarrow 15/2^-)$	2
708.2(3)	10(1)				
718.1(2)	49(2)	1.1(1)	$E2$	$(15/2^+ \rightarrow 11/2^+)$	1
729.2(3)	13(2)				
737.7(3)	17(1)	1.2(2)	$E2$	$(23/2^- \rightarrow 19/2^-)$	2
760.0(4)	7(1)				
819.5(4)	15(1)				
837.4(3)	23(1)				
860.2(5)	6(1)				
881.7(3)	23(1)	1.2(2)	$E2$	$(19/2^+ \rightarrow 15/2^+)$	1
918.9(4)	10(1)				1
938.4(4)	11(1)				
952.8(5)	6(1)				
1056.4(4)	29(2)	0.7(1)	$E1$	$(13/2^- \rightarrow 11/2^+)$	$3 \rightarrow 1$

[a]Possible doublet.

and 644 keV transitions may suggest that they are doublet transitions. Their nature, however, cannot be ascertained because of limited γ-γ statistics, i.e., are these transitions self-coincident doublets? The γ rays previously assigned to ^{109}I [4] have been reordered in the present level scheme. γ rays in coincidence with the strong 594 keV transition [see Figs. 1(b) and 1(c)] are shown in Fig. 3(a), while γ rays in coincidence with the 548 and 1056 keV transitions are shown in Figs. 3(b) and 3(c), respectively.

It was possible to produce one-dimensional proton-correlated γ-ray spectra corresponding to rings of JUROGAM detectors at constant angle θ with respect to the beam axis. Relative intensities of transitions in these spectra allowed discrimination between quadrupole and dipole character. An angular-intensity ratio R, defined as

$$R = \frac{I_\gamma(\theta = 157.6^\circ, 133.6^\circ)}{I_\gamma(\theta = 94.2^\circ, 85.8^\circ)},$$

has been extracted for the stronger transitions placed in the level scheme of ^{109}I, as listed in Table I. The results have been normalized to $R \equiv 1.0$ for the strong 594 keV transition. Assuming that this transition is of stretched quadrupole ($E2$) character, γ rays of pure stretched dipole character are then predicted to have $R \approx 0.65$, such as the 1056 keV transition linking band 3 to band 1. However, values of $R \approx 1.0$ are also expected for pure nonstretched $\Delta I = 0$ ($E1$) transitions; such an assignment is made to the 548 keV transition linking band 2 to band 1, in analogy to similar results found for the ^{111}I isotope [20,21].

IV. DISCUSSION

In order to interpret the band structures in ^{109}I and justify the present spin-parity assignments, the level scheme is compared with those of other odd-A iodine isotopes. In addition, cranking calculations are used to strengthen the proposed band structures.

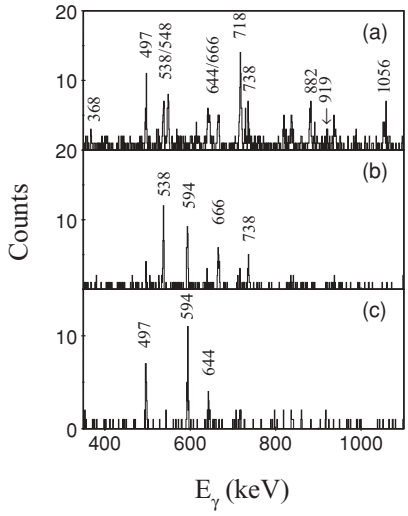

FIG. 3. γ-ray spectra (1 keV/channel) without background subtraction showing transitions in coincidence with (a) the 594 keV transition, (b) the 548 keV transition, and (c) the 1056 keV transition of ^{109}I. The transitions labeled with their energies are shown in the level scheme.

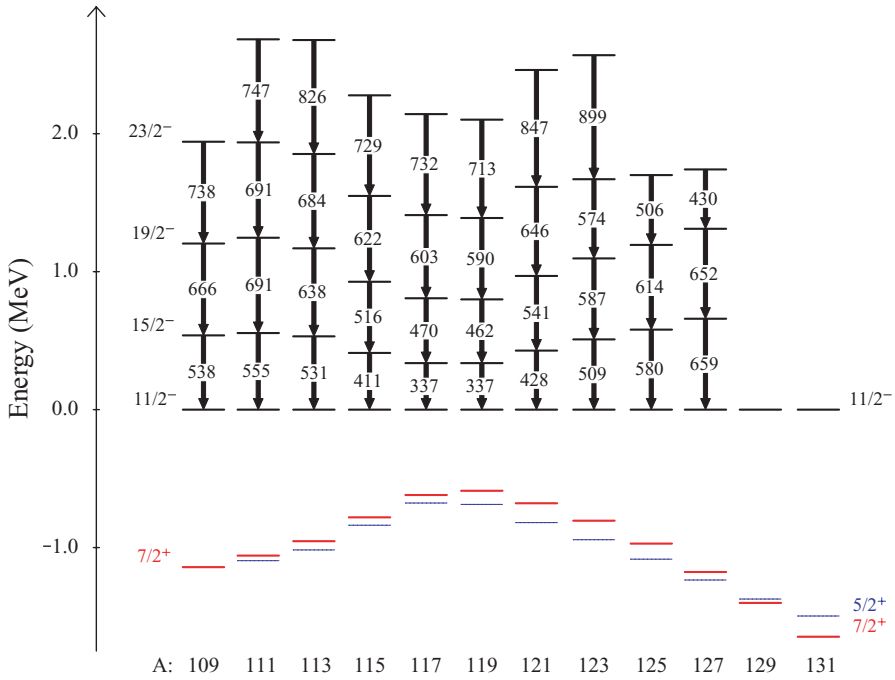

FIG. 4. (Color online) Systematics of bands built on the $\pi h_{11/2}$ orbital in odd-A iodine isotopes. The energies of low-lying $5/2^+$ (thin blue line) and $7/2^+$ (thick red line) states relative to the $11/2^-$ states are also shown. The $5/2^+$ state forms the ground state for odd-A iodine isotopes with $111 \leqslant A \leqslant 127$, while the $7/2^+$ state becomes the ground state for $A \geqslant 129$.

A. Systematics of odd-A iodine isotopes

Energy systematics of the $\pi h_{11/2}$ bands in odd-A iodine isotopes [22] are shown in Fig. 4, including the proposed ^{109}I levels. Also shown in the lower part are the relative energies of low-lying $7/2^+$ and $5/2^+$ states. The $5/2^+$ states are derived predominantly from the odd proton occupying the $2\pi d_{5/2}$ orbital and form the ground state of odd-A iodine isotopes with $111 \leqslant A \leqslant 127$. However, for $A \geqslant 129$ the ground state is based on a $7/2^+$ state derived predominantly from the $1\pi g_{7/2}$ orbital. Maximum quadrupole deformation is achieved in the odd-A iodine isotopes for $N = 64, 66$, namely ^{117,119}I, which lie midway between the $N = 50$ and $N = 82$ shell closures. Low-lying $11/2^-$ states, derived from the first $\pi h_{11/2}$ intruder orbital, are found in these isotopes. Moving away from the midshell, the relative energy of the $\pi h_{11/2}$ orbital is seen to increase, reflecting a decrease in quadrupole deformation. In addition, the relative energy of the $5/2^+$ ($\pi d_{5/2}$) and $7/2^+$ ($\pi g_{7/2}$) states decreases for isotopes moving away from the midshell. Indeed for the heavy odd-A iodine isotopes above ^{127}I ($N \geqslant 76$), the $7/2^+$ state becomes the ground state. The relative energy of the $5/2^+$ and $7/2^+$ states again decreases as neutrons are removed, and the systematics of Fig. 4 suggest that the $5/2^+$ and $7/2^+$ states in ^{109}I must lie very close in energy, and could even be inverted such that the $7/2^+$ state becomes the ground state, analogous to ^{129}I.

We propose that band 1 in ^{109}I is associated with the $\pi g_{7/2}$ orbital (supported by cranking calculations discussed in Sec. IV B below), while band 2 is based on the $\pi h_{11/2}$ intruder orbital. Indeed, the excitation energy of the bandhead of band 2 fits well into the systematics (see Fig. 4). Moreover, the ratio of the energies of the second and first excited states of band 2 fits well into the systematics of nuclei in this neutron-deficient region. Such systematics are shown in Fig. 5 for the ratio $(E_2 - E_0)/(E_1 - E_0)$ in $_{52}$Te, $_{53}$I, $_{54}$Xe, and $_{55}$Cs isotopes; the data are taken from Ref. [22]. For the even-even isotopes of tellurium and xenon, E_0 corresponds to the energy of the 0^+ ground state ($\equiv$0), E_1 to the energy of the first excited state (2^+), and E_2 to the second excited state (4^+). For the odd-A iodine and cesium isotopes, the analogous energies E_0, E_1, and E_2 correspond to the energies of the $11/2^-$, $15/2^-$, and $19/2^-$ states, respectively, of bands built on a decoupled $\pi h_{11/2}$ proton orbital. The ratio obtained for the $N = 56$ Te, I, and Xe isotones is systematically lower than the ratio obtained for the $N = 58$ isotones.

Another interesting fact is that the $15/2^- \rightarrow 11/2^-$ and $19/2^- \rightarrow 15/2^-$ transitions in ^{109}I are *lower* in energy than the corresponding transitions in ^{111}I (see Fig. 4). This may suggest that ^{109}I possesses a larger quadrupole deformation than expected when approaching the $N = 50$ shell closure. Indeed similar conclusions have been drawn for the ^{110}Xe [14] and ^{112}Xe [23] isotopes.

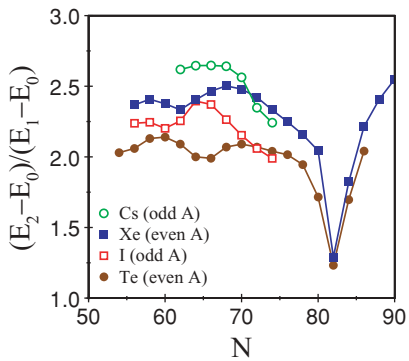

FIG. 5. (Color online) Energy-ratio systematics of the first three states in the ground-state bands of even-A Te and Xe isotopes, and the $\pi h_{11/2}$ bands of odd-A I and Cs isotopes.

The lowest state of Fig. 2 is assigned $7/2^+$ ($\pi g_{7/2}$). It is not clear whether this represents the ground state of ^{109}I or not, given the expected closeness of $5/2^+$ and $7/2^+$ levels from systematics. The nature of the ground state of ^{109}I can, however, be inferred from the properties of the proton radioactivity, namely, the Q value and mean lifetime of the decay; both are sensitive to the ℓ value (orbital angular momentum) of the decaying state, i.e., is the ground state of ^{109}I based on an $\ell = 2$ ($d_{5/2}$) or $\ell = 4$ ($g_{7/2}$) orbital? Recent theoretical work [24–27] on (axial) deformed proton emitters supports $\ell = 2$ for the level from which the proton escapes, and hence $5/2^+$ for the ground state of ^{109}I. It was not possible to observe any γ ray decaying from the $7/2^+$ state of Fig. 2 into the presumed $5/2^+$ ground state, which is consistent with the expected closeness of these two levels. Furthermore, no band structure associated with the $5/2^+$ state could be identified because of limited γ-γ statistics.

B. Woods-Saxon cranking calculations for ^{109}I

Deformation self-consistent cranking calculations based on the total-Routhian surface (TRS) formalism [28–30], employing a triaxial Woods-Saxon single-particle potential [31,32], have been performed for various (multi)-quasiparticle configurations in ^{109}I; some results are shown in Fig. 6. Single-quasiparticle levels have also been calculated as a function of rotational frequency ω. In all of these calculations, the pairing strength has been calculated at zero frequency and is modeled to decrease with increasing rotational frequency, such that it has fallen by 50% of its initial value at $\omega = 0.70$ MeV/$\hbar$, as detailed in Ref. [29]. The labeling of orbitals adopted in this paper is shown in Table II.

Average deformations, calculated at a rotational frequency 0.325 MeV/$\hbar$, are listed in Table III for the lowest one- and three-quasiparticle configurations. Moderate quadrupole deformation, $\beta_2 = 0.143$–0.183, with some degree of triaxiality $\gamma = 9^\circ$–21°, is found. It is also evident that the occupation of proton and/or neutron $h_{11/2}$ intruder orbitals tends to increase the quadrupole deformation β_2.

1. Bands 1 and 2

Single-quasiparticle levels for both protons and neutrons are plotted in Fig. 7 as a function of rotational frequency, using the

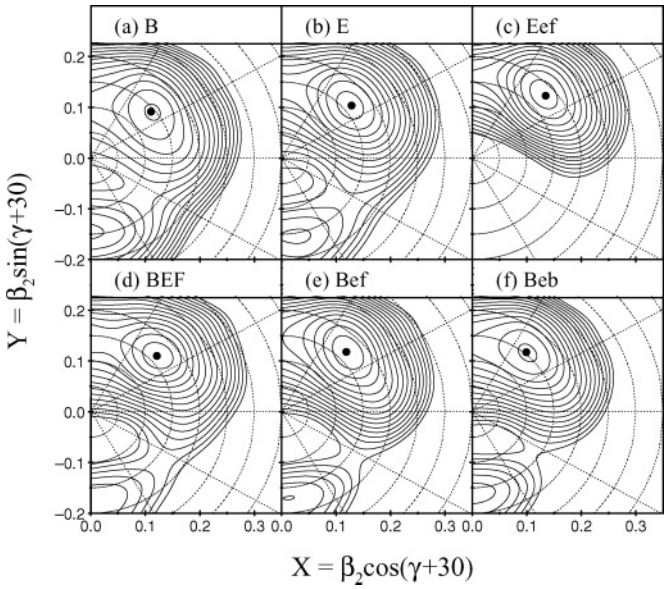

FIG. 6. TRS surfaces calculated for various one- and three-quasiparticle configurations in ^{109}I at a rotational frequency of 0.325 MeV/$\hbar$. The energy contours are separated by 250 keV.

average TRS deformation and pairing parameters appropriate for the B proton configuration (predominantly $\pi g_{7/2}$) of Table III. It can be seen that the B orbital, with signature $\alpha = -1/2$, lies lowest in energy up to $\omega \approx 0.35$ MeV/$\hbar$; hence this orbital is associated with band 1 of Fig. 2. Band 2 is then formed by a quasiparticle excitation from the B orbital into the E ($\pi h_{11/2}$) intruder orbital.

In order to corroborate these assignments, experimental alignments i_x and Routhians e' [33] are shown in Fig. 8 as a function of rotational frequency. These quantities were extracted using a variable moment-of-inertia reference with Harris parameters [34] $\mathcal{J}_0 = 2.7\hbar^2\,\mathrm{MeV}^{-1}$ and $\mathcal{J}_1 = 70\hbar^4\,\mathrm{MeV}^{-3}$ extracted from band 1. Clearly ^{109}I is not a good rotor, which is to be expected given the low predicted quadrupole deformation parameters of Table III. Nevertheless, the average experimental alignments of band 1 ($i_x \sim 2.5\hbar$) and band 2 ($i_x \sim 5.5\hbar$) are consistent with those expected for the theoretical B ($\pi g_{7/2}$) and E ($\pi h_{11/2}$) orbitals of Fig. 7(a); the theoretical alignment is simply related to the slope of the

TABLE II. Labeling of single-quasiparticle orbitals adopted in this paper.

(Parity, signature)	Protons		Neutrons	
	Label	Dominant shell-model state	Label	Dominant shell-model state
(+, +1/2)	A	$g_{7/2}$	a	$g_{7/2}$
(+, −1/2)	B	$g_{7/2}$	b	$g_{7/2}$
(−, −1/2)	E	$h_{11/2}$	e	$h_{11/2}$
(−, +1/2)	F	$h_{11/2}$	f	$h_{11/2}$

TABLE III. Average TRS deformations calculated for various configurations in ^{109}I.

Configuration	(Parity, signature)	β_2	β_4	γ
B	(+, −1/2)	0.143	0.040	10°
E	(−, −1/2)	0.165	0.042	9°
Eef	(−, −1/2)	0.183	0.042	12°
BEF	(+, −1/2)	0.162	0.042	12°
Bef	(+, −1/2)	0.165	0.042	15°
Beb	(−, +1/2)	0.154	0.042	20°
Eeb	(+, +1/2)	0.165	0.042	21°

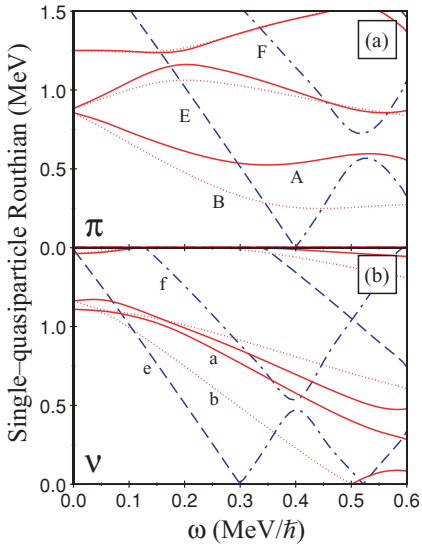

FIG. 7. (Color online) Representative single-quasiparticle positive-parity (red) and negative-parity (blue) proton (a) and neutron (b) levels calculated with a cranked Woods-Saxon potential with deformation parameters $\beta_2 = 0.143$, $\beta_4 = 0.040$, and $\gamma = 10^\circ$, and pairing parameters $\Delta_\pi = 0.68$ MeV and $\Delta_\nu = 1.10$ MeV. The parity and signature (π, α) of the levels are: (+, +1/2), solid lines; (+, –1/2), dotted lines; (–, –1/2), dashed lines; and (–, +1/2), dot-dashed lines.

quasiparticle trajectories, i.e., $i_x = -de'/d\omega$.

It can be seen in Fig. 7(a) that two positive-parity proton orbitals are near-degenerate at $\omega = 0$. These orbitals are derived from predominantly $\pi g_{7/2}$ and $\pi d_{5/2}$ states, respectively. The present Woods-Saxon calculations predict that at zero frequency, these states lie very close in energy, of the order

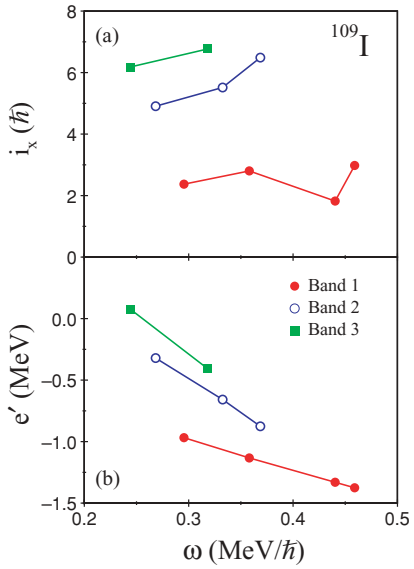

FIG. 8. (Color online) Experimental alignments (a) and Routhians (b) of the bands in ^{109}I.

of only a few 10 keV apart. The lower lying $5/2^+$ state has appreciable $\ell = 2$ components, while the $7/2^+$ state is dominated by $\ell = 4$ components. Slight changes in quadrupole deformation, especially triaxiality, can, however, invert the ordering of the $5/2^+$ and $7/2^+$ states in ^{109}I. Since the characteristics of the proton radioactivity of ^{109}I favor emission from an $\ell = 2$ state, a $5/2^+$ assignment is expected for the ^{109}I ground state. However this ground state must lie very close to the $7/2^+$ state of Fig. 2.

2. *Band 3*

The experimental alignment of band 3 in Fig. 8(a) is seen to be $\sim 1\hbar$ higher than band 2 and is consequently too high to correspond to a pure single-quasiparticle configuration. The TRS calculations of Fig. 6 suggest that three-quasiparticle configurations become important for frequencies $\omega \approx 0.325$ MeV/$\hbar$. In particular, the Beb configuration, of predominantly $\pi g_{7/2} \otimes \nu(h_{11/2} g_{7/2})$ character, is predicted to be the lowest three-quasiparticle configuration in energy. Hence this negative-parity structure could be a candidate for band 3 and indeed has the appropriate $\alpha = +1/2$ signature required for the $I^\pi = (13/2^-)$ bandhead assignment. However, the theoretical alignment of this three-quasiparticle configuration, obtained from the slopes of the B, e, and b orbitals of Fig. 7, is much higher ($i_x \sim 9.5\hbar$) than the experimental value of Fig. 8(a) ($i_x \sim 6.5\hbar$). In addition, the experimental Routhian (excitation energy in the rotating frame) of band 3 in Fig. 8(b) is too low for a three-quasiparticle structure. Furthermore, no three-quasiparticle configurations have been identified in any odd-A iodine isotopes at such low spin and excitation energy.

An alternative interpretation is therefore warranted for band 3. The core nuclei (even Te isotopes) of the odd-A iodine isotopes are well known to exhibit quadrupole vibrational collectivity [12], i.e., a 2^+ phonon. Furthermore, nuclei of this mass region close to $N = Z = 56$ exhibit octupole collectivity (3^- phonon). Indeed, octupole collectivity has been discussed in ^{108}Te [35], the core of ^{109}I, in addition to several other light $_{52}$Te and $_{54}$Xe isotopes; see Ref. [36] and references therein. Coupling of single-particle states to vibrational phonons, both quadrupole and octupole, has also been discussed in the case of odd-A $_{53}$I isotopes [37]. Octupole collectivity has also been recently discussed in ^{111}I [21].

In the even Te isotopes, the 4_1^+ state occurs at approximately twice the energy of the 2_1^+ state, i.e., these nuclei appear vibrational, and the 2_1^+ and 4_1^+ states correspond to one and two quadrupole-vibrational phonons, respectively. The neutron-deficient even Te isotopes also exhibit low-lying negative-parity sidebands that decay to the ground-state bands via strong $E1$ transitions. This has been taken as evidence for octupole collectivity in these nuclei, whereby an octupole-vibrational phonon (3^-) mixes with negative-parity two-quasiparticle configurations. The pure one-phonon 3^- state is difficult to observe, especially in the very light even Te isotopes because of the difficulty in producing these exotic nuclei. However, the corresponding 3^- state has recently been identified in ^{114}Xe using the exceptional sensitivity of the EUROBALL spectrometer including the observation of an $E3$ transition

decaying directly to the ground state [38]. A 3^- state has also been proposed in ^{112}Xe [23]. Systematics suggest that the one-phonon 3^- state should exist at an excitation energy of $\sim$1.6 MeV. In odd-A nuclei, it is possible to couple the odd particle to the collectivity of the core. In regard to octupole collectivity, such features are well established in the heavy Rn-Ra-Th (mass 220) region [39,40].

An intriguing possibility is that band 3 in ^{109}I represents a similar coupling of the odd proton, residing in a $\pi g_{7/2}$ orbital, to a collective octupole-vibrational phonon of the ^{108}Te core. With the odd proton in this orbital, both proton and neutron $h_{11/2}$ and $d_{5/2}$ orbitals, with $\Delta j = \Delta \ell = 3$, are available to induce the octupole collectivity. The coupling of a 3^- octupole-vibrational phonon to a $\pi g_{7/2}$ orbital yields spin and parity $I^\pi = 13/2^-$, consistent with the present bandhead assignment of band 3. The relative excitation energy of bands 1 and 3 of 1.65 MeV represents the excitation energy of the phonon, and this value is consistent with the excitation energy expected from systematics. The octupole-vibrational phonon should generate an alignment of $3\hbar$ [39]. The alignment plot of Fig. 8(a) indeed shows that the alignment of band 3 ($\pi g_{7/2} \otimes 3^-$) is 3–4$\hbar$ higher than band 1 ($\pi g_{7/2}$).

V. CONCLUSION

A new level scheme has been constructed for the proton-unbound nucleus ^{109}I following a recoil-decay-tagging experiment using the JUROGAM and GREAT spectrometers. It has been possible to extend relative proton single-particle energies, namely, $\pi g_{7/2}$ and $\pi h_{11/2}$ states, to the extremes of isospin close to the $N = Z = 50$ nucleus ^{100}Sn.

ACKNOWLEDGMENTS

The authors thank Drs. R. Wyss and W. Nazarewicz for providing the Woods-Saxon cranking codes. This work has been supported by the EU Sixth Framework Programme "Integrating Infrastructure Initiative—Transnational Access," Contract No. 506065 (EURONS) and by the Academy of Finland under the Finnish Centre of Excellence Programme 2006–2011 (Nuclear and Accelerator Based Physics Programme at JYFL). It has also been supported in part by the U.K. Engineering and Physical Sciences Research Council, the Swedish Science Research Council, and the Göran Gustafsson Foundation.

[1] J. Skalski, Phys. Lett. **B238**, 6 (1990).
[2] W. Nazarewicz, G. A. Leander, and J. Dudek, Nucl. Phys. **A467**, 437 (1987).
[3] E. S. Paul *et al*., Phys. Rev. C **51**, 78 (1995).
[4] C. -H. Yu *et al*., Phys. Rev. C **59**, R1834 (1999).
[5] R. S. Simon *et al*., Z. Phys. A **325**, 197 (1986).
[6] C. W. Beausang *et al*., Nucl. Instrum. Methods Phys. Res. A **313**, 37 (1992).
[7] M. Leino *et al*., Nucl. Instrum. Methods Phys. Res. B **99**, 653 (1995).
[8] M. Leino, Nucl. Instrum. Methods Phys. Res. B **126**, 320 (1997).
[9] R. D. Page *et al*., Nucl. Instrum. Methods Phys. Res. B **204**, 634 (2003).
[10] I. H. Lazarus *et al*., IEEE Trans. Nucl. Sci. **48**, 567 (2001).
[11] P. Rahkila, Nucl. Instrum. Methods Phys. Res. A (to be published).
[12] B. Hadinia *et al*., Phys. Rev. C **72**, 041303(R) (2005).
[13] B. Hadinia *et al*., Phys. Rev. C **70**, 064314 (2004).
[14] M. Sandzelius *et al*., Phys. Rev. Lett. **99**, 022501 (2007).
[15] J. Blachot, Nucl. Data Sheets **107**, 355 (2006); and references therein.
[16] T. Faestermann *et al*., Phys. Lett. **B137**, 23 (1984).
[17] P. J. Sellin *et al*., Phys. Rev. C **47**, 1933 (1993).
[18] C. Mazzocchi *et al*., Phys. Rev. Lett. **98**, 212501 (2007).
[19] D. C. Radford, Nucl. Instrum. Methods Phys. Res. A **361**, 297 (1995); **361**, 306 (1995).
[20] E. S. Paul *et al*., Phys. Rev. C **61**, 064320 (2000).
[21] P. Spolaore *et al*., Nucl. Phys. **A682**, 387c (2001).
[22] Brookhaven National Nuclear Data Center: http://www.nndc.bnl.gov/ensdf/
[23] J. F. Smith *et al*., Phys. Lett. **B523**, 13 (2001).
[24] E. Maglione, L. S. Ferreira, and R. J. Liotta, Phys. Rev. Lett. **81**, 538 (1998).
[25] E. Maglione, L. S. Ferreira, and R. J. Liotta, Phys. Rev. C **59**, R589 (1999).
[26] D. S. Delion, R. J. Liotta, and R. Wyss, Phys. Rev. Lett. **96**, 072501 (2006).
[27] D. S. Delion, R. J. Liotta, and R. Wyss, Phys. Rep. **424**, 113 (2006).
[28] W. Nazarewicz, G. A. Leander, and J. Dudek, Nucl. Phys. **A467**, 437 (1987).
[29] R. Wyss, J. Nyberg, A. Johnson, R. Bengtsson, and W. Nazarewicz, Phys. Lett. **B215**, 211 (1988).
[30] W. Nazarewicz, R. Wyss, and A. Johnson, Nucl. Phys. **A503**, 285 (1989).
[31] W. Nazarewicz, J. Dudek, R. Bengtsson, T. Bengtsson, and I. Ragnarsson, Nucl. Phys. **A435**, 397 (1985).
[32] S. Cwiok, J. Dudek, W. Nazarewicz, W. Skalski, and T. Werner, Comput. Phys. Commun. **46**, 379 (1987).
[33] R. Bengtsson and S. Frauendorf, Nucl. Phys. **A327**, 139 (1979).
[34] S. M. Harris, Phys. Rev. **138**, B509 (1965).
[35] G. J. Lane *et al*., Phys. Rev. C **57**, R1022 (1998).
[36] E. S. Paul *et al*., Phys. Rev. C **76**, 034323 (2007).
[37] S. V. Jackson, W. B. Walters, and R. A. Meyer, Phys. Rev. C **11**, 1323 (1975).
[38] G. de Angelis *et al*., Phys. Lett. **B535**, 93 (2002).
[39] J. F. C. Cocks *et al*., Phys. Rev. Lett. **78**, 2920 (1997).
[40] J. F. C. Cocks *et al*., Nucl. Phys. **A645**, 61 (1999).